Structural behaviour of steel ropes subjected to heavy thermal transients simulating fire scenarios

V.Fontanari, B.D. Monelli
DIMTI University of Trento, via Mesiano 77– 38121 Trento, e-mail: vigilio.fontanari@unitn.it

F. Degasperi
SIF-LaTIF, Via Provina 24 – 38040 Trento,Italy, e-mail: fabio.degasperi@provincia.tn.it

A. Dallago, *SIF-PAT,* Via Brennero, 136 38100 Trento, Italy

Abstract

In this paper a methodology for determining the fire resistance of metallic wire ropes for ropeways and civil applications is presented. The problem has been faced by means of a numerical-experimental approach, focusing on the development of a simulation tool for the assessment of the rope response to heavy thermal transients resembling a fire scenario (ISO 834 standard temperature curve). To this purpose a Finite Element (FE) parametric model was built up, suitable for simulating the thermo-mechanical response of a wire rope. The numerical predictions about load redistribution among wires during the test and rope's collapse conditions, allowed for safely carrying out the experimental fire characterizations of both full locked and strand ropes. The experimental results are in optimal agreement with numerical simulations thus allowing to consider the proposed methodology suitable for the analysis of the most diffused wire ropes configurations.

Keywords: metallic wire ropes, fire resistance, damage scheme, standard ISO 834 curve, FEM

INTRODUCTION

The serious accidents occurred in the Alps in the winter season 2000/01 (Kaprun 2000, Zugspitze 2001) pointed out the lack of technical knowledge regarding the wire ropes behaviour in case of fire. As reported by Oplatka [1], who carried out an extensive analysis of recent fire accidents involving ropeways, the rope usually collapse in a relatively short time. This problem is even emphasised by the ever increasing diffusion of ropes in civil buildings, bridges and cable car.
The rope exposure to high temperature implies a rapid worsening of the wire's mechanical behaviours. The steel used for producing wires has a fine perlitic microstructure, characterized by an heavy hardening level which is responsible for the very high mechanical properties [2-4], Unfortunately, at a temperature higher than 300°C, the dislocation structure start to evolve determining an irreversible decrease of the mechanical strength. For temperatures higher than 600°C a recristalization process can take place producing a new crystallographic texture [5-8]. For long time exposure at relatively high temperatures creep phenomena can occur. However recristallization and creep contribution to the rope collapse can be excluded in case of fire due to the relatively short time of the event.
In the scientific and technical literature there is a lack of information on the rope behaviour during fire: the high costs of the experiments and the difficult set up of the experimental devices still represent a strong obstacle towards the acquisition of experimental results on different classes of ropes. It is therefore necessary to refer to papers and standards concerning the assessment of civil structures, which suggest different time-temperature histories to simulate the fire behaviour of the structure. The ISO 834 standard (fig. 1), which aims to simulate the time-temperature evolution in closed environments surrounding the structure during a fire accident [9-11], is one of the most frequently adopted approaches. The structure loaded to the 'in service' typical condition is monitored up to the final collapse or to the loosening of its functionality (i.e. excessive deformation incompatible with structural integrity). The ISO 834 temperature curve overestimates of the fire heaviness: only the flash over phase is considered whereas the combustion initiation as well as the expansion phases, during which the temperature increase more slowly, are neglected. It is very difficult to transfer these concepts in the study of ropes behaviour. The ropes response and the thermal history of each single wire are hardly valuable during the fire transient.

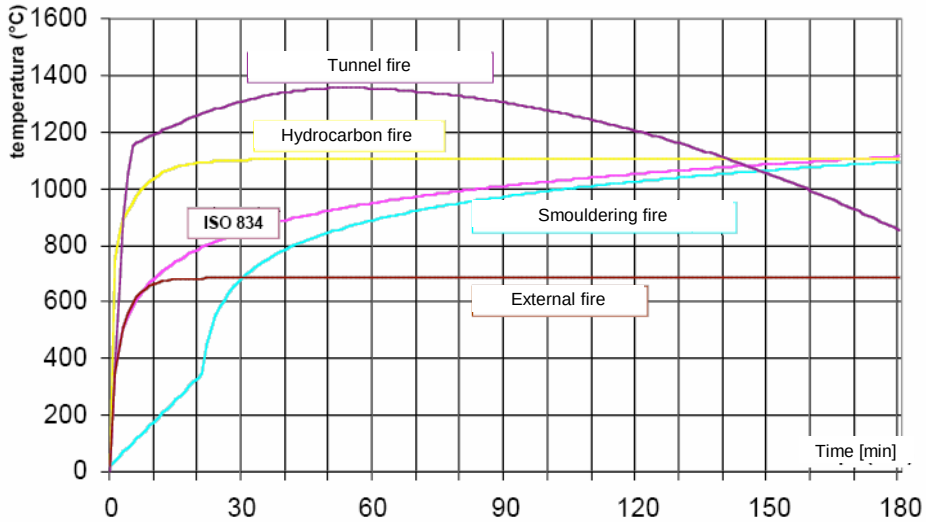

Figure 1 Comparison among ISO 834 and other common time temperature histories (EN 1993 1-2).

In scientific literature a great effort has been spent to understand the mechanical behaviour of wire ropes under different loading condition, whereas no theoretical, numerical or experimental contribution can be found dealing with the mechanical behaviour of ropes during heavy thermal transients. In particular, several numerical and analytical models have been proposed with the aim of predicting loads sharing interaction among wires [2,12]. It has to be noted however that even though analytical models can predict the load distribution among wires, they are unfortunately unable to correctly describe the rope behaviour when subjected to heavy in service loading because of the complex phenomena such as contact, friction, plasticity and large displacements (full-slip regime vs. no-slip regime), which noticeably influence the mechanical response [13-25]. In order to face the analysis of these phenomena some numerical approaches based on the Finite Element (FE) Method have been successfully adopted [13-16].
In the present paper a numerical-experimental approach is developed for studying the mechanical behaviour of wire ropes undergoing to heavy thermal loads simulating a fire accidents. The principal aim is to define a design tool for predicting the response of different classes of ropes. To this purpose a parametric FE model was manufactured, which allowed for the simulation of the rope's thermo-mechanical history during the fire transient following the ISO 834 standard. The FE analysis is very important for defining the experimental set up for carrying out experiments under safe conditions. The model has been validated on the basis of experimental data measured on the rope and on single wires: tensile tests at room temperature are used for defining the mechanical model whereas thermal histories measured in different positions of the rope and the surrounding environment are used to build up the thermal model. Moreover, in order to correctly simulate the mechanisms of load redistribution among wires during the thermal transient, an extensive campaign is carried out on single wires to build up a data base of wires $\sigma-\varepsilon$ curves at different temperatures. These stress strain curves are used as input for the FE model for simulating the thermal transient of the rope subjected to 'in service' axial loading. The FE modelling of the thermo-mechanical response of the rope allowed to predict the load redistribution, the collapse mechanisms and the time to collapse at high temperature. The method represents the basis for defining a general purpose predictive tool suitable for studying different types of ropes usually adopted in ropeways and cable-structures.

1. WIRE ROPE'S CONFIGURATION

The study is focused both on full-locked and strand ropes. In particular, two specific geometrical configurations were considered: a 124 wires full-locked rope with a nominal diameter of 60 mm and a 186 wires Warrington-Seale 6x31 strand rope with a nominal diameter of 36 mm.

1.1 The full-locked rope

The rope is characterised by a central straight wire, three layers of circular wires with alternate right-left lay and by three external layers of Z shaped wires also with right-left lay [fig. 2]. These ropes are typically used

for cable-structures. The wires have higher cross sectional areas as compared to wires for cableways ropes, that have to be characterised by lower flexural stiffness. The effective cross section of the studied rope is nearly 2485 mm^2, with a filling coefficient (ratio between effective and nominal cross section area) of nearly 88%. The chemical composition of steel wires is reported in table 1.

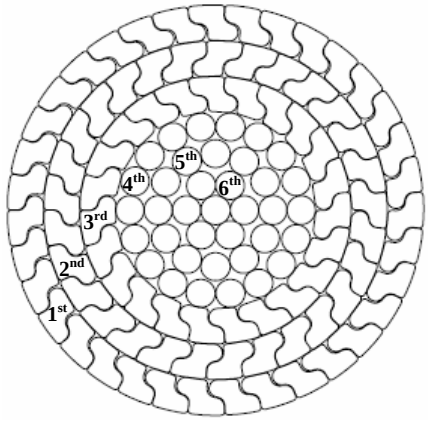

	N° wires	Φ / H [mm]	Cross section [mm^2]
Core straight wire	1	Φ 4.26	14.24
Sixth layer	6	Φ 4.09	13.14
Fifth layer	12	Φ 4.09	13.14
Fourth layer	18	Φ 4.09	13.14
Third layer	23	H 5.20	22.5
Second layer	29	H 5.20	23.2
First layer	35	H 5.20	23.2

(ϕ=circular wires diameter, H=thickness of Z shaped wires)

Figure 2 Geometry of the locked rope 60 [1 + 6 + 12 + 18 + (23 + 29 + 35) Z];

Elem.	C	Mn	S	P	Si	Sn	Cu	Al	Mo	Ni	Cr	V
%	0.825	0.725	0.003	0.013	0.215	0.02	0.02	0.029	0.003	0.016	0.12	0.066

Table 1 – Chemical composition of the steel wires

1.2 The Warrington-Seale strand rope

The rope configuration is labelled as 6x31WS+SF, made up by 6 Warrington-Seale strands each one of 31 wires and a polimeric inner core (PPC). The 12+6/6+6+1 strand cross section and the double helical winding configurations are schematically presented in fig. 3.

(a)

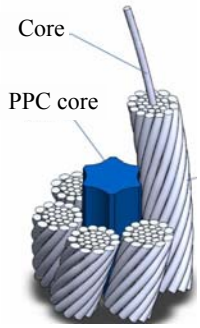

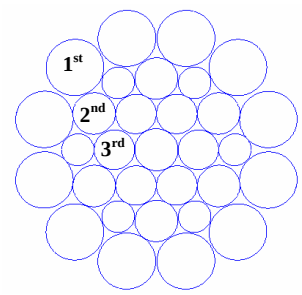

(b)

Strand

Diameter (mm): 15.3

Helical pitch (mm): 90

Wire diameters (mm):

1	2.06
6	1.92
6/6	1.56-2.20
12	2.70

Figure 3 a) 6x31 WS configuration b) cross section of the WS strand 12+6/6+6+1.

1.3 Mechanical properties of the wires

The remarkable differences in the cross sections affect the mechanical strength of wires. An extensive experimental characterization was carried out to evaluate the effects of drawing operation. To this purpose, 12 specimens were tested for each wire type, using a servo-hydraulic testing machine (Instron 8516 100 kN). Strain was determined by means of an extensometer with *gauge length* of 12.5 mm. The specimens were extracted from the ropes. The representative true stress true strain curves are plotted in figures 4 and 5.

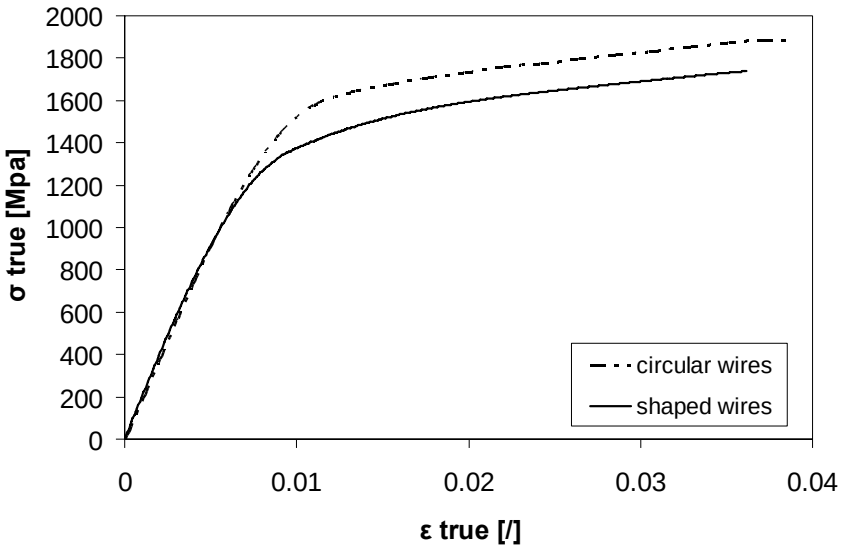

Figure 4 Full-locked rope ∅60**:** true stress-true strain curves of circular and shaped wires.

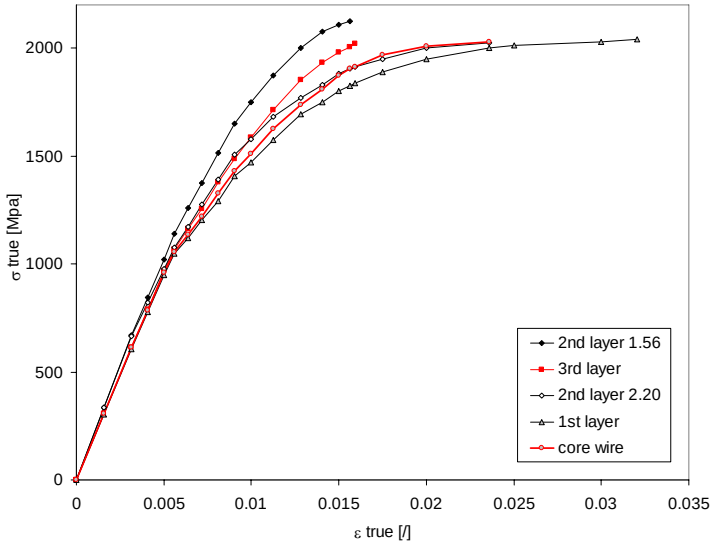

Figure 5 Strand rope 6x31WS: true stress-true strain curves of circular and shaped wires

1.4 The tensile behaviour of the full locked rope

The tensile test on the rope was performed on a servo-hydraulic 10MN testing machine. An extensometer with a gage length of 1 m was applied on the rope. Several loading cycles within the load range between 5% and 50% of the estimated fracture load were applied in order to reach a stabilization of wires contacts. After this preliminary phase the rope presented an initial linearly elastic behaviour which allowed for determining an apparent Young modulus of nearly 141 GPa. The extensometer was removed at the onset of non-linear behaviour, load was then increased up to the rope failure and the engineering strain was estimated on the basis of the gripping heads position control. In figure 5 the load vs. nominal strain are plotted.

1.5 The tensile behaviour of the WS strand and the 6x31 WS strand rope

The tests on the WS strand and on the 6x31 WS strand rope were performed on the same testing machine but the specimens were not brought to failure. The tests were stopped at nearly 80% of the theoretical failure load in order to preserve the extensometer. In this way the comparison with the FE analysis can be extended to a large part of the stress strain curve of the rope. The WS strand showed a linear behaviour up to a load of nearly 150 kN and a corresponding elastic modulus of 175 GPa. Above this load a non linear behaviour was observed. An apparent elastic modulus of 136 GPa was calculated for the rope. In fig. 6 the curves load vs. nominal strain for the WS strand and of the 6x31 WS strand rope are plotted.

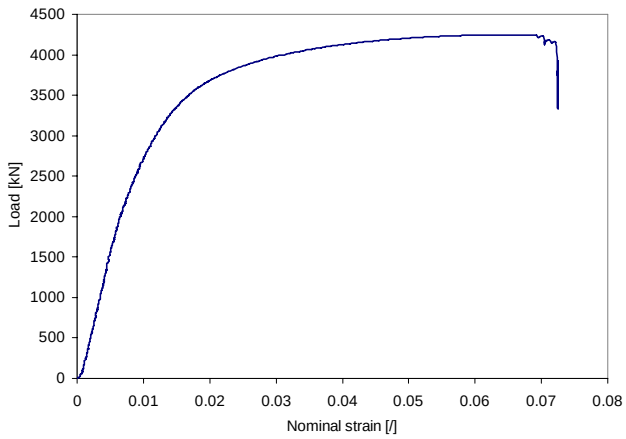

a)

b)

Figure 6 a) room temperature load vs. strain curve of the full locked rope; b) the broken rope before removal from the Instron frame.

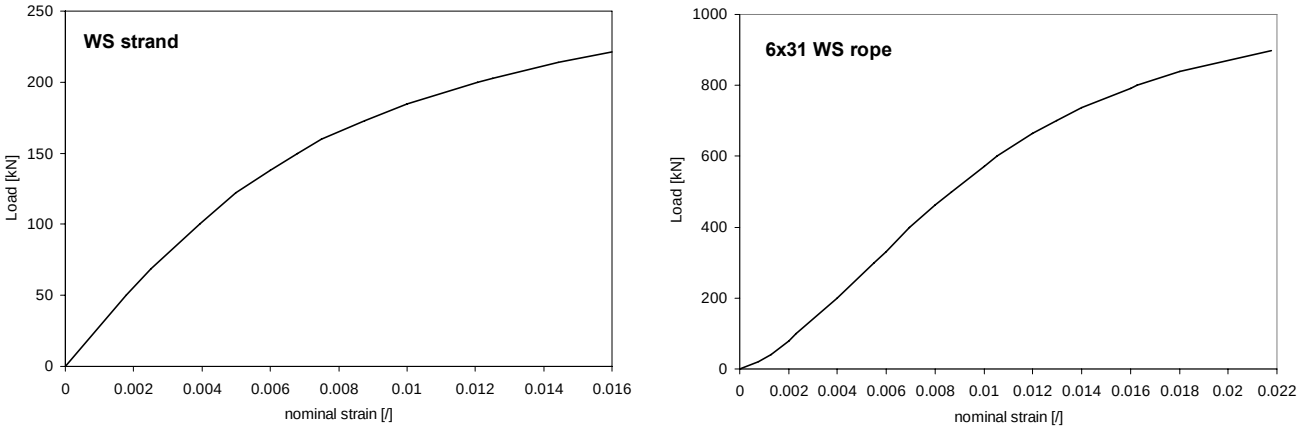

Figure 7. Load vs. strain curves for the WS strand and for the 6x31WS rope

2. FINITE ELEMENT ANALYSIS OF THE ROPE'S STRUCTURAL BEHAVIOUR

The finite element modelling was performed using the Ansys Rel.11 code. Only an excerpt of the rope was modelled in order to cope with computational heaviness of the analysis. Parametric solid models were built to enable the possibility of extending the analysis to ropes having different dimensions. Eight nodes brick elements were used to build up the model, whereas the contact between wires was modelled using s*urface to surface* gap elements. The theoretical analyses of Costello and Feyer [12,2] stated that for axially loaded rope the relative displacements between wires are negligible, as a consequence friction does not play a relevant role on the stress strain evolution into the specimen. As a consequence frictionless contact was implemented. Homogeneous, isotropic materials models, following the J_2 flow criterion and the isotropic hardening rule were assumed and the experimental tensile *true stress-true strain* σ-ε curves were associated to the corresponding wire in the strand. Axial loading was implemented in the FE models by imposing an axial displacements on a cross sectional end, whereas the circumferential displacements were constrained in order to prevent the rotation of the strands about their longitudinal axis. As observed in service, an axial twisting moment arises. The value of this moment is however small due to the alternate lay up of the wire layers.

2.1 Finite element model of the full locked rope

The model is built up by a central straight wires, three inner spiral strands of circular wires with right handed- left-handed alternate lay and finally three external layers of shaped wires also with right-handed-left handed alternate lay (fig. 8). The axial length of the model was chosen as a consequence of a compromise

between the needs of limiting the computational heaviness and of avoiding any perturbation due to boundary effects. The elements sizes were determined by means of a convergence analysis. In order to limit the computational effort, an iterative procedure was set up to identify the contact surfaces and to minimize the number of contact pairs. A picture of the final mesh and an example of the surface of possible contact between two wires, as identified by the iterative procedure is shown in figure 9.

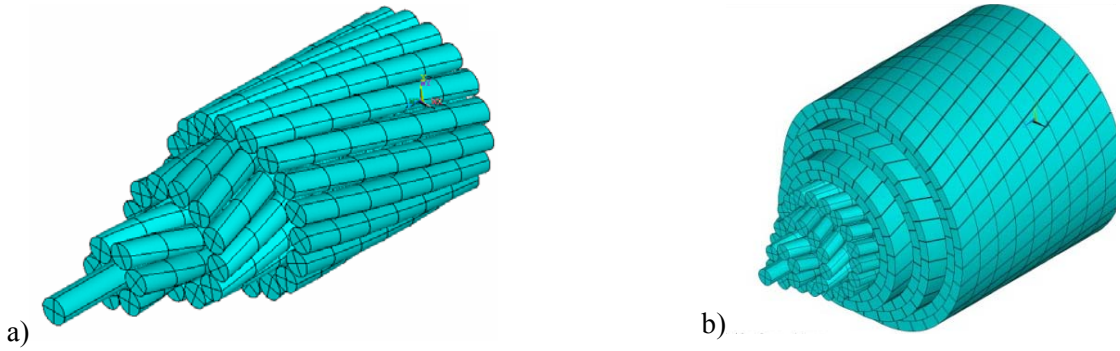

Figure 8. a) inner core with alternate lay-up, b) solid model of the rope.

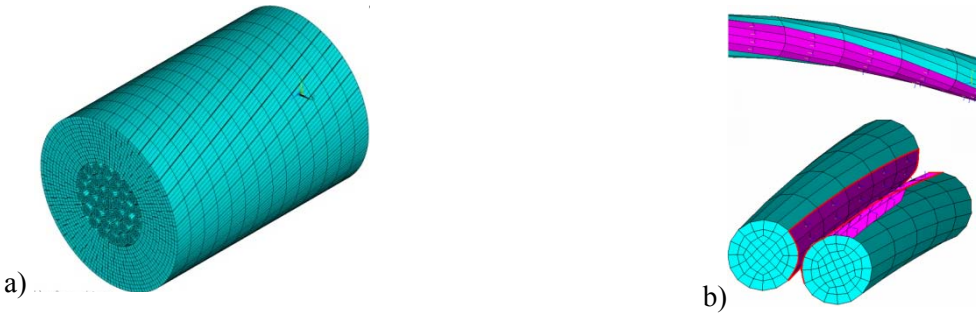

Figure 9 a) mesh of the rope excerpt, b) identification of the contact pairs

2.2 FE model of the WS strand and of the 6x31 WS rope

Due to the outstanding geometrical complexity of strand ropes and to the very high number of wires, the length of the FE model has to be limited as far as possible. To this purpose a preliminary analysis was performed on a simpler strand (6+1) and validated by comparing its results with the predictions of the theoretical model of Costello [12]. In this way it was possible to demonstrate that perturbation due to boundary constraints are negligible for a model length at least equal to 1/16 of the helical pitch. Moreover the 8-noded brick should have a characteristic dimension lower than 1/12 of the wire radius elements in the radial direction and 1/10 of the pitch in the axial direction. The WS strand 12-6/6-6-1 was built up following the suggestion coming from this preliminary analysis. The FE model is plotted in fig. 10.

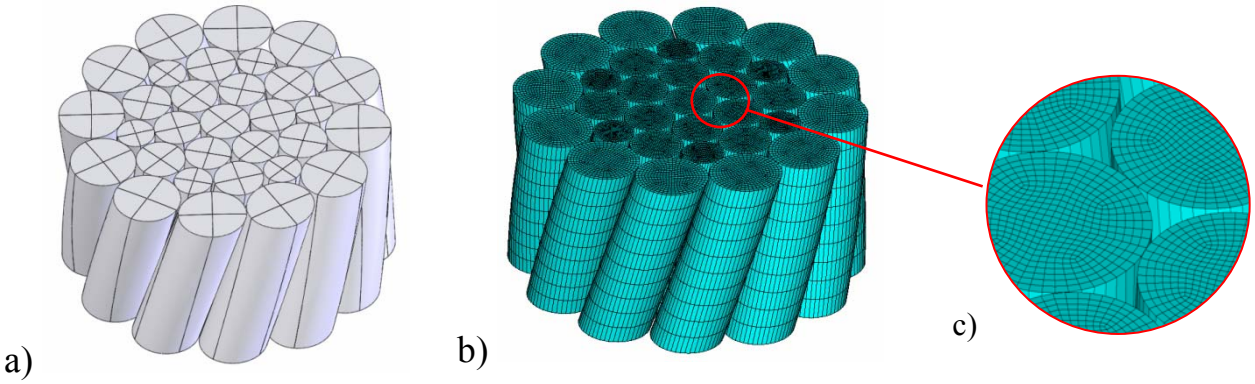

Figure 10 Warrington-Seale strand 12-6/6-6-1: (a) solid model, (b) mesh (c) detail of the mesh

The model for the 6x31 strand rope can be manufactured by considering that each strand is made by wires, which are wound, conforming to an helix (secondary helix) having a pitch of 90 mm, around the core wire

that is shaped following another helical trajectory (principal helix) (fig. 11 a). The mesh refinement is the same as that used for the 6+1 WS strand. The polymeric inner core was modelled by means of a surface which does not contribute to carry the axial load and acts only as a radial support for the strands.
The final mesh adopted for the analysis is plotted in fig. 11 b).

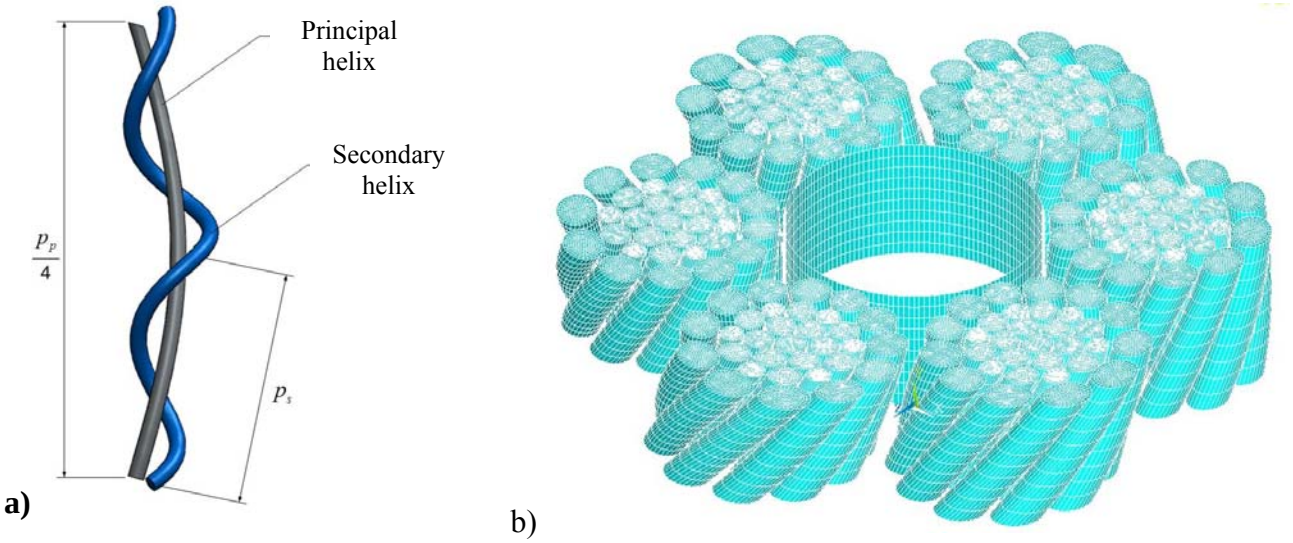

Figure 11 6x31WS strand rope: a) double helical winding of a single wire, b) FE model**.**

2.3 FE models validation

The FE models were used to simulate the tensile tests previously described. For the full locked rope the comparison can be made for the first part of the σ–ε curve up to the point at which the extensometer was removed. For the WS strand and the strand rope the extensometer was not removed during the test and the ropes were loaded up to the 80% of their nominal strength. The experimental and numerical curves are plotted for comparison in fig. 12-13, in table 2 the numerical and experimental values of the elastic modulus are collected.

	Full locked rope		WS 12-6/6-6-1 strand		6x31 WS rope	
	Experimental	FE	Experimental	FE	Experimental	FE
Elastic Modulus (GPa)	141	143	175	172	136	134.5

Table 2 – Comparison between FE and experimental apparent elastic moduli for the different rope's configurations.

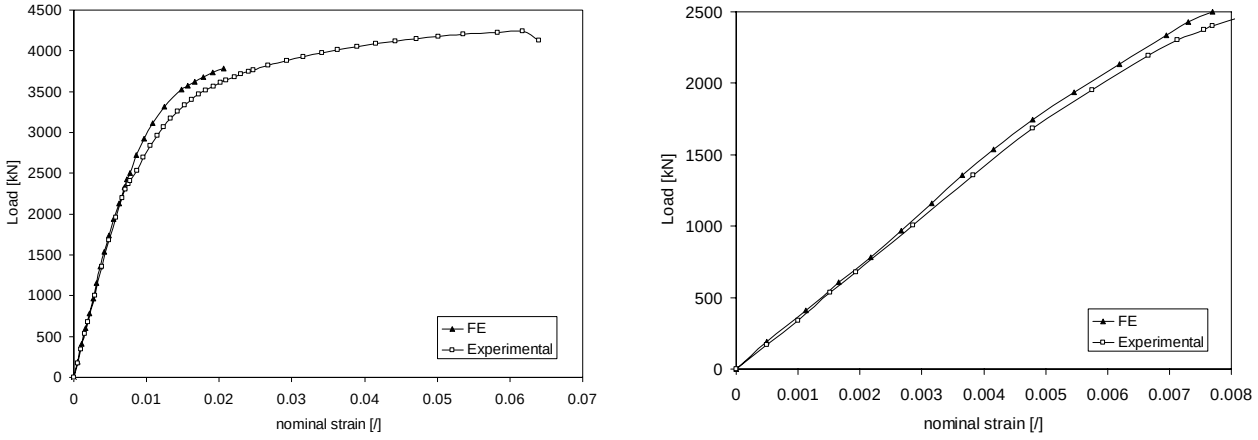

Figure12 Full locked rope ∅60: a) comparison between experimental and FE tensile curves, b) detail on the elastic part of the curves.

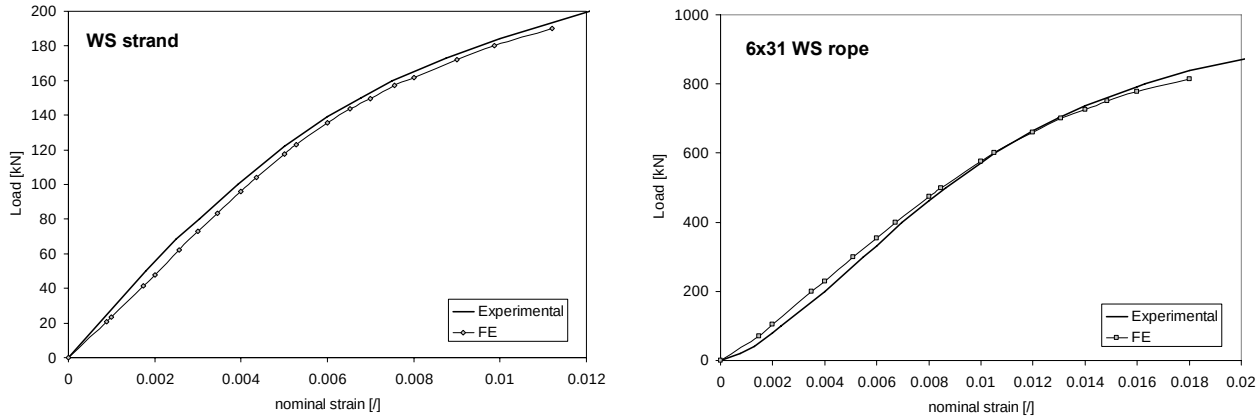

Figure 13 Comparison between experimental and FE tensile curves: a) WS strand 12-6/6-6-1; b) 6X31 WS rope

The FE analysis correctly reproduces the first part of the experimental curve of the full locked rope. After the extensometer's removal the rope engineering strain was calculated on the basis of the gripping heads displacements, thus overestimating the rope compliance. For this reason a progressive shift between experimental and numerical results (fig. 12 a) was observed. In the initial part of the curve (fig. 12 b). the relative differences between numerical and experimental values are always within 2%. A similar agreement was found for the WS strand and the 6x31 WS rope, being the relative differences always within 1.5%. It can be concluded that the FE model is capable of simulating the evolution of the wire's behaviour which determines the ropes mechanical response.

3. FINITE ELEMENT ANALYSIS OF THE ROPE THERMAL BEHAVIOUR

The ISO 834 time-temperature history will be generated in a specifically designed oven mounted into the 10 MN testing machine. A FE thermal model able to simulate the thermal transient in the oven has to be developed. The short thermal transient allows for disregarding the any creep damage since the rope collapses as a consequence of the thermal decay of wires mechanical behaviours. It is therefore of paramount importance to correctly know the thermal transient of each wire of the rope, since this can have a strong influence on the load redistribution among wires. A thermocouple in the rope's core, four thermocouples on the rope's skin with angular spacing of 90°, and finally four thermocouples in the oven chamber to measure the environments temperature were adopted. The measured temperature profiles are plotted in fig. 14a).

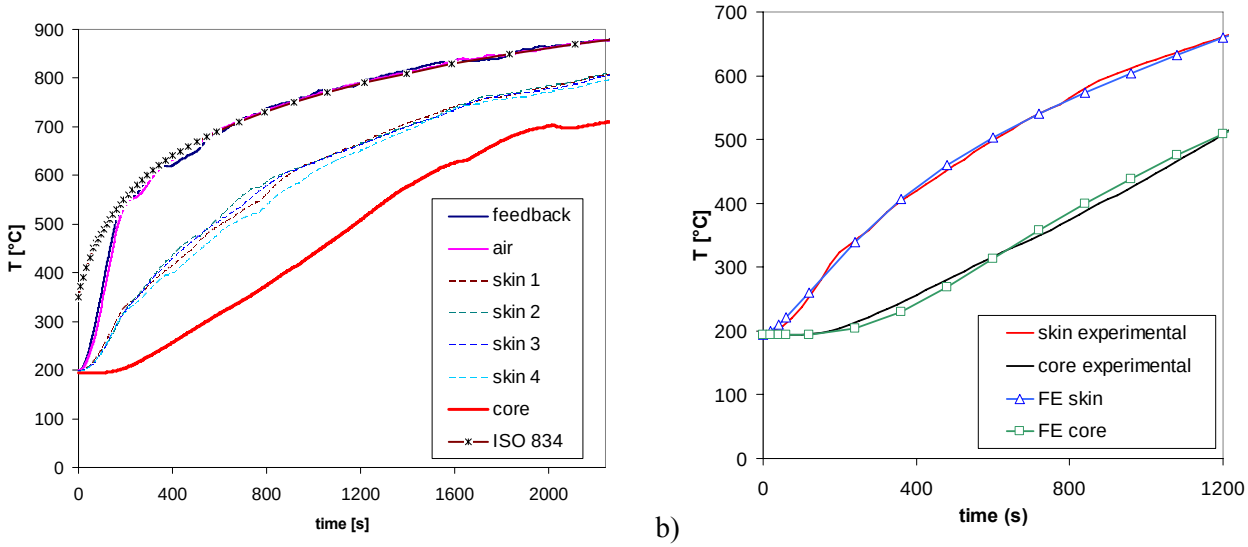

a) b)

Figure 14 a) experimental time temperature profile measured in different points of the oven, b) comparison between numerical and experimental results.

The thermocouples labelled '*feedback*' and *'air 1'* positioned in the centre of the oven chamber point out that the ISO 834 temperature profile is linked after nearly 3 minutes and then the curve is followed quite satisfactorily. The thermal transients measured by the four thermocouples on the rope's skin are overlapped thus showing that the temperature field is axi-symmetric and a radial heat flux toward the rope core can be assumed with reasonable approximation. The temperature ramp measured by the core thermocouple follows with a certain delay (nearly 3 minutes) the other curves. As a consequence the temperature gap between skin and core is noticeable in the central part of the curve representing the transient time-temperature history, this can have very important influence in distinguishing the wires behaviours during the test. The FE calibration was carried out by iteratively setting some parameters: the global heat transfer coefficient between air and rope skin, the contact heat resistance between shaped wires layers and finally the contact heat transfer resistance between circular wires of the internal strands. On the basis of the experimental measurements and introducing the material thermal properties that were found in the literature [5,6,17,18], an optimal reproduction of the thermal transient of each wire's layer can be obtained (fig. 14b).

4. MECHANICAL PROPERTIES OF THE WIRES AT DIFFERENT TEMPERATURES

The mechanical behaviour of wires are strongly dependent on the local temperature. Even though the steel grade adopted for wire ropes is quite common, systematic information on its mechanical properties as a function of temperature are not available. It is therefore necessary to collect a data base of experimental stress-strain curves based on tests carried out on wires segments extracted from the rope at different temperatures after different stabilization time intervals. Tests were performed on a 100 kN servo hydraulic testing machine provided with a heat furnace suited for testing materials at temperatures up to 1000 °C. The temperatures and stabilization times were selected to comply with the typical time-temperature histories experienced by each wire during the fire simulation. Preliminary tests showed that shaped wires behave like circular wires when tested at T>300 °C. The experimental campaign was then focused on wires with circular section and the tests were performed at temperatures ranging from 100°C to 600 °C with steps of 100 °C. With reference to the expected fire resistance of the rope, particular care was devoted to get the temperature steady before to start the test. Two stabilization time ranges were considered: the shorter one was fixed to 3 min., whereas the longer one was nearly 8 min. In fig. 15 the σ–ε curves obtained at different testing temperatures and stabilization times are plotted.

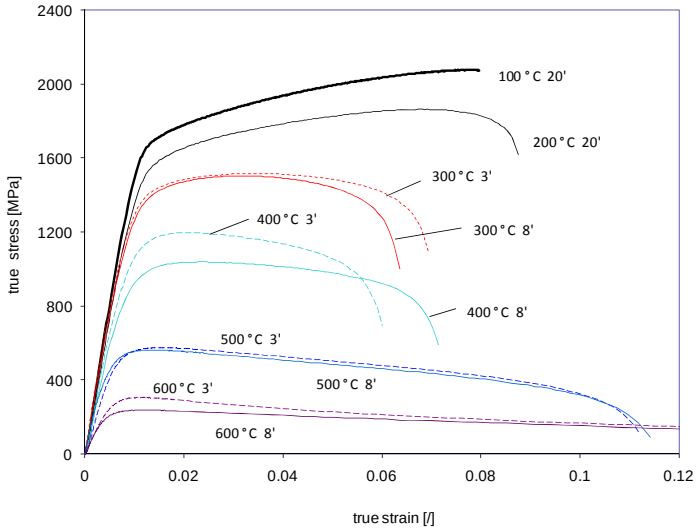

Fig. 15: σ–ε curves at different temperatures and for different stabilizing time intervals

The values of Young modules, yield strength, ultimate tensile strength deduced from the curves are summarized in table 3. For the tests performed at 100° and 200° C negligible effects were observed on material response. At higher temperatures the dependence on time is distinguishable. The maximal difference can be observed for tests carried out at about 400 °C. At lower temperatures the kinetics for microstructural modification is slow and longer exposition time should have been applied. On the contrary at higher temperatures the kinetics becomes very fast and the annealing phenomena occur in very short time intervals.

T [°C]	E [GPa]	$\sigma_{y,stab\ 2'}$ [MPa]	$\sigma_{y,stab\ 8\text{-}10'}$[MPa]	$\sigma_{R,stab\ 2'}$[MPa]	$\sigma_{R,stab\ 8\text{-}10'}$[MPa]
20	186	1560	1560	1885	1885
100	169	1630	1630	2078	2078
200	157	1490	1490	1864	1864
300	140	1280	1320	1503	1517
400	125	1055	890	1196	1039
500	110	510	505	575	563
600	87	285	214	306	238

Table 3: results of the tests carried out at different temperatures on circular wires

5. STUDY OF THE ROPES TENSILE RESPONSE DURING THE FIRE TRANSIENT

5.1 The thermo-structural FE model.

The FE model previously described and validated by the structural and thermal analyses was adopted to model the rope behaviour when subjected, under 'in service' loading, to the ISO 834 time temperature history. The tensile behaviours of the wires measured at different temperatures were implemented in the FE model. Since material behaviour depends also on the exposure time, two analyses were performed using the tests results obtained for the two stabilization times. The corresponding times to rope collapse can represent respectively the lower and the upper limit of the ropes fire resistance. The boundary conditions of the rope are similar to those previously described for the tensile test. The 'in service' nominal stress (nearly 30% of the ultimate tensile strength of the rope) was applied at room temperature (T=20°C), then the thermal transient was started and the axial load was maintained constant. Each wire layer is forced to follow its temperature history as previously measured (fig. 16).

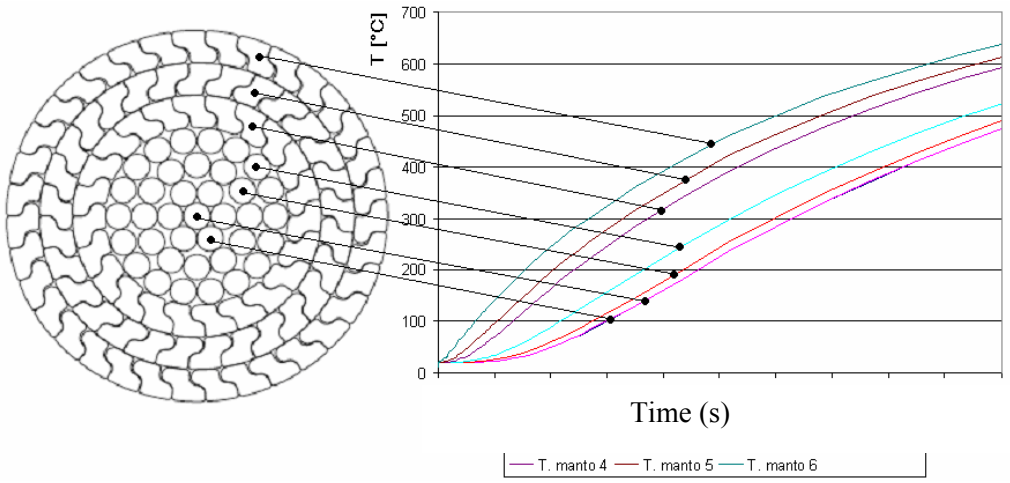

Figure 16: time-temperature curves applied to the different wire layers.

5.2 FE modeling of the full locked rope fire resistance

In figure 17 the ropes nominal strain evolution with time is plotted for the two simulations: the lower limit is obtained by considering the materials properties of the wires corresponding to the longer stabilization time (8min.), whereas the upper limit is obtained by introducing in the FE model the materials properties corresponding to a shorter stabilization interval. The rope behaviour predicted by the two analyses is initially similar and a noticeable difference takes place when the rope approaches the final collapse. Two phase can be clearly detected: a linear strain vs. time evolution, which can be essentially explained by considering the thermal expansion of the material, followed by an ever increasing strain rate up to the final collapse. It is reasonable to assume that the experimental response of the rope will be intermediate.

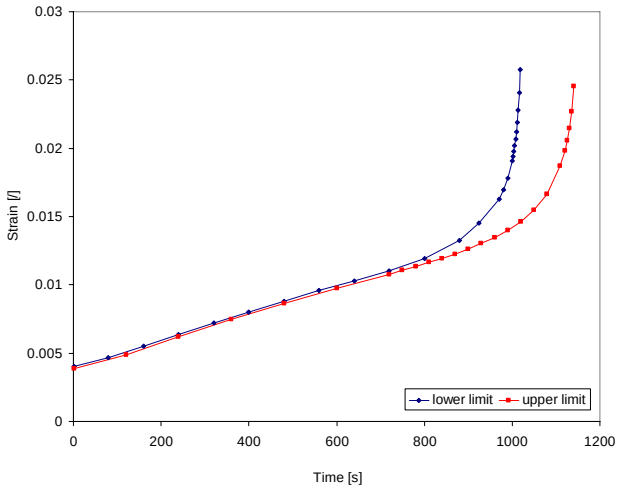

Figure 17: upper and lower limit of the nominal strain vs. time curves during fire simulation

In order to set up the experimental test it is necessary to know how the final collapse takes place. This analysis can be carried out by considering the mechanisms of load redistribution predicted by the FE analysis. With reference to the stress-strain curves plotted in figure 15, the external wire layers, which are subjected to the highest temperatures (fig. 16) undergo to extensive plastic deformation at a nearly constant, or even decreasing stress. As a consequence the load is progressively transferred towards the internal wire strands. All wires are forced to experience the same axial elongation and they fail after reaching their rupture elongation, which depends on the temperature and therefore on the radial position of the wire. It is therefore reasonable to assume that failure starts on the inner wire layers. Load is progressively transferred to the external layers, determining the rope's final collapse. The rope failure is not catastrophic, since a consistent amount of the energy is dissipated by plastic deformation of the external wire layers, which behave following the $\sigma-\varepsilon$ curves determined at nearly 600°C (fig. 10). The characteristic whip stroke experienced in the ropes tensile tests at room temperature can be strongly smoothed or even suppressed because external wires can act as a protective shield, thus mitigating the danger of the final failure. This conclusion allows to design with reasonable safety the experimental test.

5.3 The experimental behaviour of the full locked ropes

The experimental tests on the rope was performed on the 10 MN testing machine, using the heating system previously described. In order to correctly follow the ISO 834 time temperature curve the oven was preheated before to introduce the rope and to start the test. Following the standard specifications the rope was preloaded up to the 'in service' nominal load (30% of the service load) for 15 min, before to start the test, in order to obtain a mechanical stabilization. To this purpose the positioning mechanism described in fig. 18 was adopted.

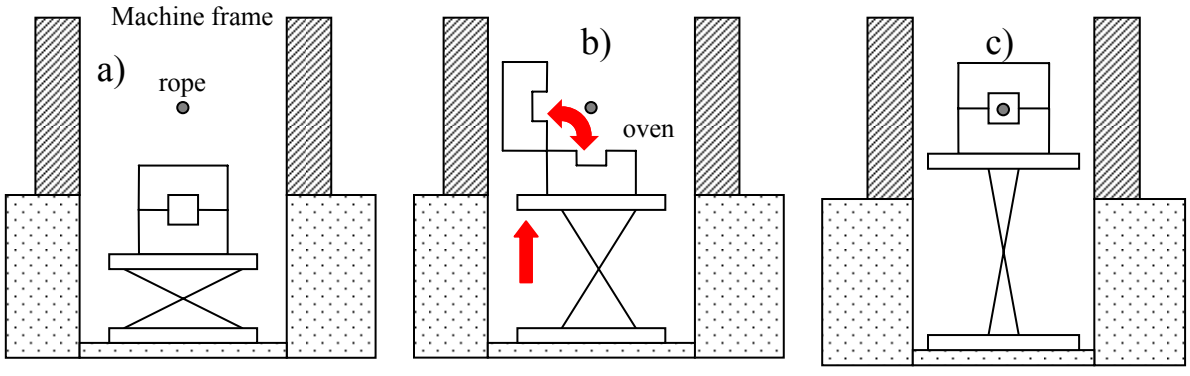

Figure 18 a) oven preheating and rope preloading b) oven positioning; c) final test configuration

Two tests on two rope's segments were performed. The obtained strain vs. time to collapse curves were nearly overlapped with a time delay at the final collapse shorter than 30 s.: the first test was terminated after nearly 18 min 30 s, the second presented a little bit longer life (nearly 19 min). In figure 18 numerical and experimental results are plotted, showing a good agreement: the FE model correctly reproduces the thermo-mechanical processes taking place in the rope when stretched to the 'in service' load and undergoing to a very heavy thermal transient. The analysis was then extended to study locked ropes with different diameter and after some adjustments adopted for studying also the WS strand ropes. In particular full locked ropes with diameters of 26 mm and 80 mm respectively were tested in order to cover the range of the most typical ropes diameter used in practical applications. The strain vs. time curves are shown in figure 19a, whereas the time to failure vs. rope diameter are plotted in fig. 19b.

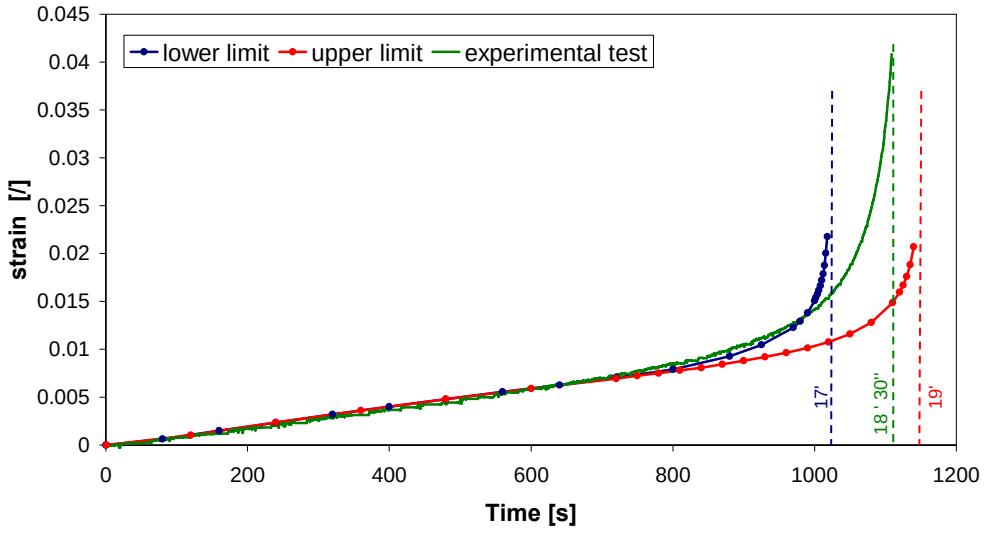

Figure 18 Comparison among strain vs. time curves predicted by FEM and obtained by experimental tests

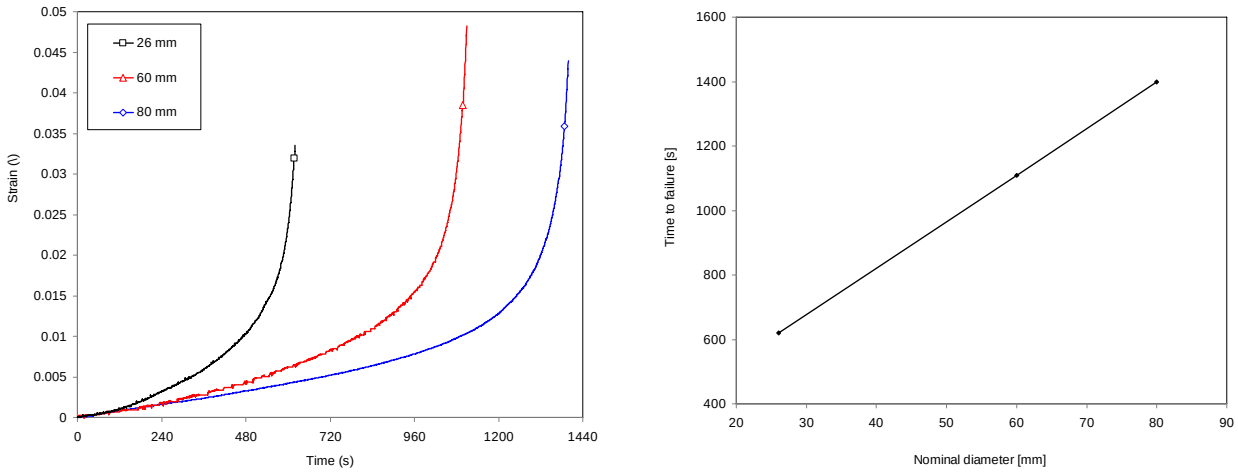

Figure 19 Full locked ropes: a) fire resistance curves for different ropes diameter; b) time to failure vs. ropes diameter

5.4 The experimental behaviour of WS strand ropes

The WS strand ropes under investigation are characterised by a polymeric core, that can have an important role on the ropes thermo-mechanical behaviour. In order to evaluate how polymer degradation takes place during the test, some preliminary tests on unloaded ropes were performed showing an initial softening followed by polymer combustion. The local temperature is influenced but the oven retrofit can reasonably maintain the ISO 834 temperature profile in the oven chamber. The fire resistance tests were then performed on four ropes having the following diameters 14, 24, 35 e 52 mm. The strain vs. time curves are shown in figure 20a, whereas the time to failure vs. rope diameter are plotted in fig. 20b. The instant at which core

combustion takes place can be appreciated in the curves. After an initial increase of the strain rate, the oven retrofit restores the ISO 834 time-temperature conditions and the ropes show a residual load bearing capability.

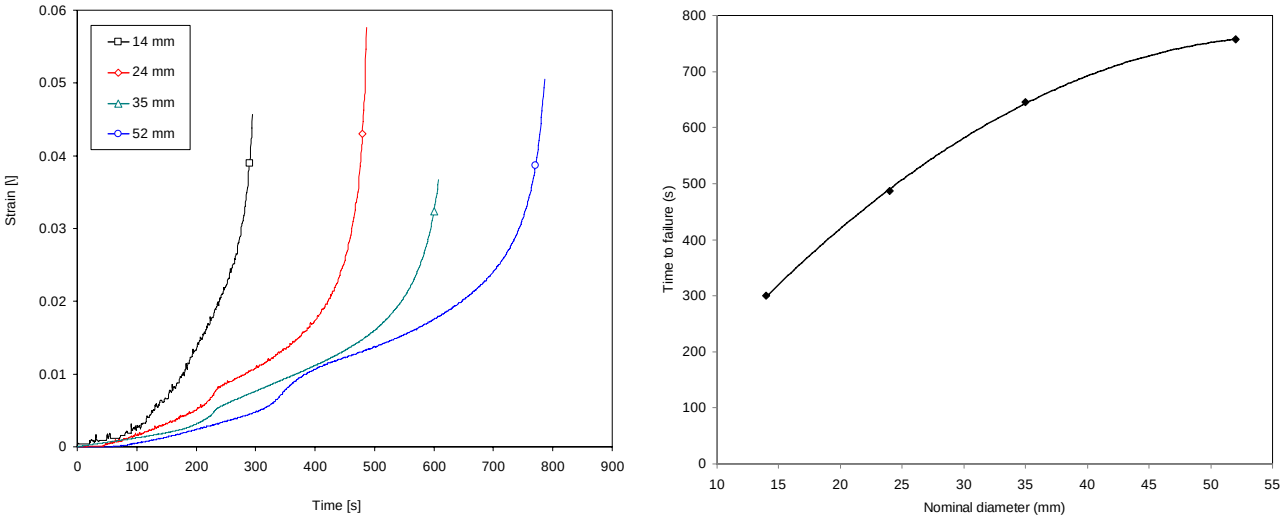

Figure 20 WS strand ropes: a) fire resistance curves for different ropes diameter; b) time to failure vs. ropes diameter

CONCLUSIONS

The proposed experimental and numerical procedure showed to be appropriate for studying the fire resistance of full locked and WS strand ropes. The FE analysis was able to correctly model the mechanical behaviour of the both full locked and strand ropes at room temperature and to predict the load redistribution among different wire layers during the test. Moreover the FE analysis correctly reproduces the thermo-mechanical processes occurring in the rope during heavy thermal transients. The thermo-mechanical analysis can be extended to all locked ropes and adapted, after some adjustments, also for studying wire strand ropes. Moreover a first database of times to failure ws. Ropes diameter was built up, which can be a starting point for defining the class of fire resistance of different type of ropes.

REFERENCES

[1] G. Oplatka, "Brand von Seilbahnen", *ISR – International Seilbahn Rundschau*, 1, 8-11, 2001

[2] K. Feyrer,: *Drahtseile Bemessung, Betrieb, Sicherheit*, Ed. Springer Verlag, 2000

[3] J. G. Wistreich, "The fundamentals of wire drawing", Metall. Rev., 1958, Vol. 3, pp. 97-142.

[4] V. Fontanari, M. Benedetti , U. Bulf , "Numerical analysis of the rolling process of shaped wires for locked steel ropes". *Journal of materials processing technology*, 170, 97-107, 2005

[5] G. E. Dieter, *Mechanical metallurgy*, Mc Graw-Hill Book Company, 1988.

[6] R. E. Reed-Hill, R. Abbaschian, *Physical Metallurgy Principles*, PWS Publishing Company, 1994.

[7] C.R. Chaplin, "Failure mechanisms in wire ropes", *Engineering failure analysis*, 2, 1, 45-57, 1995

[8] A. Ray, S. K. Dhua, K. B. Mishra, S. Jha, "Microstructural Manifestations of Fractured Z-Profile Steel Wires on the Outer Layer of a Failed Locked Coil Wire Rope", *Practical Failure Analysis*, 3, 4, 51-55, 2003

[9] A. Amico, G. Bellomia: "Meccanica dell'incendio e valutazione del rischio", *Dario Flaccovio Editore,* 2002

[10] A. Amico, G. Bellomia: "Carico di incendio e resistenza al fuoco delle strutture", *Dario Flaccovio Editore,* 2002
[11] S. Pustorino: "Sicurezza Incendio" *ETS*, 2007
[12] G. A. Costello, *Theory of Wire Rope,* New York: Ed. Springer Verlag, 1990.
[13] M. Raoof, "Design recommendations for steel cables", *Struct. Engineering Rev*., 4,223-233, 1992
[14] F. H. Hruska, "Radial forces in wire ropes", *Wire and wire products*, 27, 459-463, 1952
[15] J. Lanteigne, " Theoretical estimation of the response of helically armored cables to tension, torsion and bending", *Journal of Applied Mechanics*, 52, 423-432, 1985
[16] D. Elata, R. Eshkenazy, M.P. Weiss, "The mechanical behaviour of a wire rope with an independent wire rope core", *Int. J. of Solids and Structures*, 41, 1157-1173, 2004
[17] S. A. Velinsky, G. L. Anderson, G. A. Costello, "Wire rope with complex cross sections", J. of Engng. & Mech. Div. ASCE, 110, 380-391, 1984.
[18] J. W. Phillips, G. A. Costello, "Analysis of wire ropes with internal wire ropes cores", *Transaction ASME*, 52, 510-516, 1985
[19] R. C. Wang, W. M. McKewan, "A model for the structure of round-strand wire ropes", *O.I.P.E.E.C. Bulletin*, vol. 81, pp. 15-42, 2001
[20] G. A. Costello, R. E. Miller, "Lay effect of wire rope", J. Engng. & Mech. Div. ASCE, 105, 4, 597-608, 1979.
[21] C. Jolicoeur, A. Cardou, " A numerical comparison of current mathematical models of twisted wire cables under axisymmetric loads", *J. of Energy Res. Tech.*, 113, 241-249, 1991
[22] M. Raoof, I. Kraincanic, "Prediction of coupled axial/torsional stiffness coefficients of locked coil ropes", *Computers & structures*, 69, 305-319, 1998
[23] W. G. Jiang, J. L. Henshall, J. M. Walton, "A concise finite element model for three-layered straight wire rope*", Int. J. of Mech. Science*, 42, 63-86, 2000
[24] K.H. Wehking, S. Ziegler, "Berechnung eines einfachen Seils mit FEM", *Draht*, 5, 32-36, 2003
[25] M. Giglio, A. Manes, "Life prediction of a wire rope subjected to axial and bending loads", *Engineering Failure analysis*, 12, 549-568, 2005
[26] ASM, 'ASM Handbook vol. 1', *ASM Metals Park OHIO*, 1998
[27] P.L. Dowling, J.E. Harding, R. Bjorhovde: "Constructional steel design – an international guide", Elsevier applied science, 1992
[28] V. Fontanari, B. D. Monelli, F. Degasperi, "Experimental and numerical analysis of locked coil ropes fire behavior", *Proceedings of 2009 SEM Annual Conference & Exposition on Experimental and Applied Mechanichs*, Albuquerque, New Mexico, 2009.